



CHORUS

This is the accepted manuscript made available via CHORUS. The article has been published as:

Combination of first-principles molecular dynamics and XANES simulations for LiCoO_2 -electrolyte interfacial reactions in a lithium-ion battery

Tomoyuki Tamura, Masanori Kohyama, and Shuji Ogata

Phys. Rev. B **96**, 035107 — Published 5 July 2017

DOI: [10.1103/PhysRevB.96.035107](https://doi.org/10.1103/PhysRevB.96.035107)

Combination of first-principles molecular dynamics and XANES simulations for LiCoO₂-electrolyte interfacial reactions in a Li-ion battery

Tomoyuki Tamura,^{1,2,*} Masanori Kohyama,³ and Shuji Ogata¹

¹*Department of Physical Science and Engineering,*

Nagoya Institute of Technology, Nagoya, 466-8555, Japan

²*Center for Materials research by Information Integration (CM²),*

Research and Services Division of Materials Data and Integrated System (MaDIS),

National Institute for Materials Science (NIMS), Tsukuba 305-0047, Japan

³*Research Institute of Electrochemical Energy (RIECEN),*

Department of Energy and Environment,

National Institute of Advanced Industrial Science

and Technology (AIST), Ikeda 563-8577, Japan

(Dated: June 13, 2017)

Abstract

We performed a first-principles molecular dynamics (FPMD) simulation of the interfacial reactions between a LiCoO₂ electrode and a liquid ethylene-carbonate (EC) electrolyte. For configurations during the FPMD simulation, we also performed first-principles Co *K*-edge XANES (X-ray absorption near-edge structure) simulations, which can properly reproduce the bulk and surface spectra of LiCoO₂. We observed strong absorption of an EC molecule on the LiCoO₂ {110} surface, involving ring opening of the molecule, bond formation between oxygen atoms in the molecule and surface Co ions, and emission of one surface Li ion, while all the surface Co ions kept Co³⁺. The surface Co ions having the bond with an oxygen atom in the molecule showed remarkable changes in simulated *K*-edge spectra, which are similar to those of the *in-situ* observation under electrolyte soaking (D. Takamatsu *et al.*, *Angew. Chem. Int. Ed.* 51 (2012) 11597). Thus the local environmental changes of surface Co ions due to the reactions with an EC molecule can explain the experimental spectrum changes.

I. INTRODUCTION

Rechargeable Li-ion batteries (LIBs) with high energy density are indispensable components for new electric motorization, while significant improvement of cycle durability is essential for the long time usage in electric vehicles. It is well known that there exist reaction barriers for Li ions to pass through electrode-electrolyte interfaces, depending on the kinds of electrode and electrolyte materials and on the status of surfaces or interfaces. These barriers seriously affect the degradation of LIBs. Thus it is important to investigate detailed reactions at the electrode-electrolyte interface during the charge-discharge cycle so as to understand the degradation mechanism.

For this purpose, *in-situ* nano-scale characterization techniques have been extensively developed.¹ X-ray absorption spectroscopy (XAS) has become increasingly important for the structural and chemical characterization of electrode materials and their changes in LIBs. In the case of transition-metal oxide cathode materials, the X-ray absorption near-edge structures (XANES) is able to provide sensitive information on chemical bonding, valence states, and coordination around a target atom. Recently, *in-situ* *K*-edge XANES has been applied to clarify valence changes of transition-metal ions in Li-rich solid-solution layered cathode material $\text{Li}_2\text{MnO}_3\text{-LiAO}_2$ ($A=\text{Co, Ni, etc}$) during the charge-discharge process, in order to understand the high capacity mechanism of this material.² *In-situ* observation using total-reflection fluorescence XAS (TRF-XAS) has been also applied to identify the chemical reactions at the interface between a LiCoO_2 electrode and a liquid electrolyte as a mixture of ethylene carbonate (EC) and diethyl carbonate (DEC).³ LiCoO_2 is a typical cathode material, frequently used in LIBs in these two decades. Significant changes in Co *K*-edge XANES spectra were observed by electrolyte soaking, and it was concluded that the reduction of Co^{3+} ions occurred within a depth of a few nanometers from the surface of the electrode, based on theoretical estimation of high concentration of anti-site Co ions on the Li sites caused by a very low oxygen chemical potential due to the contact with the liquid electrolyte.³

On the theoretical side, first-principles molecular dynamics (FPMD) simulations based on density-functional theory (DFT) for electrode-electrolyte interfaces in LIBs should be very effective to clarify possible interfacial reactions, although computational costs of such FPMD simulations are very large. Recently, FPMD simulations have been applied to anode-

electrolyte interfaces so as to investigate the solid-electrolyte interphase (SEI) formation by using supercomputers,⁴⁻⁶ while few FPMD simulations have been applied to cathode-electrolyte interfaces. In addition, first-principles XANES simulations based on DFT can successfully reproduce transition-metal *K*-edge spectra⁷⁻¹⁰ as applied to cathode materials in LIBs.¹¹⁻¹⁴ Thus theoretical XANES simulations should be effective in interpreting experimental XANES spectra about structural or chemical changes around transition-metal ions in cathode materials in contact with a liquid electrolyte. If this approach is combined with FPMD simulations to obtain realistic interfacial reactions or configurations, we could obtain quite reliable data to be directly compared to the experimental spectra. This combination can be referred to as *in-situ* first-principles XANES simulation.

For theoretical XANES spectra of Co *K*-edge, Koyama *et al.*¹² systematically evaluated the spectra of pristine LiCoO₂ of various polymorphs and Li-removed CoO₂, and showed that the energies of the peaks and shoulders are strongly dependent on the local structure even with the same chemical formula or the same oxidation state. Okumura *et al.*¹⁴ simulated Co *K*-edge spectra of Li_{1-x}CoO₂ during the actual Li deintercalation process including some phase transitions, and showed that the highest peak moved to the high-energy position by oxidation of Co³⁺ to Co⁴⁺ while the second highest position was maintained. These theoretical studies focused on spectral changes in the oxidation reaction of Co³⁺ to Co⁴⁺ in LiCoO₂, while few theoretical studies dealt with spectral changes in the reduction reaction of Co³⁺ to Co²⁺. As mentioned above, significant changes in the *K*-edge XANES spectra for surface Co ions, observed by the *in-situ* TRF-XAS of LiCoO₂ in contact with a liquid electrolyte, were attributed to the reduction of Co³⁺ to Co²⁺, supposing local configurations rich in anti-site Co ions on Li sites, in ref 3. However, there is no discussion on realistic atomic configurations or their stability for LiCoO₂ surfaces containing reduced Co ions. There is also no discussion on realistic processes of formation of reduced Co ions in contact with the electrolyte. Furthermore, there has been no direct theoretical examination of the XANES spectra from such configurations in contact with the electrolyte, which should be compared with the experimental results.

In the present study, we perform FPMD simulations for the interface between a LiCoO₂ cathode and a liquid EC electrolyte in order to clarify chemical reactions at this interface. Then, we perform first-principles Co *K*-edge XANES simulations for interface configurations during the FPMD simulation, which can reveal the spectrum changes by the chemical

reactions at the interface. We show that our *in-situ* theoretical XANES simulation can provide deeper insights and alternative interpretation for the results of *in-situ* experimental observation.³

II. COMPUTATIONAL DETAILS

The present calculations are performed by using computational code QMAS¹⁵ to implement projector-augmented wave (PAW) calculations^{16–18} with the generalized gradient approximation (GGA)¹⁹ for the exchange-correlation energy functional. GGA+ U ²⁰ with the effective Hubbard- U parameter $U_{\text{eff}} = U - J = 5.0$ eV for Co $3d$ orbitals is adopted. The plane-wave energy cutoff is set to 544 eV (=40Ry). 1s electrons of Li are dealt with as valence electrons owing to the semicore nature. FPMD simulations are performed in a NVT ensemble with the time-step width of 1.2 fs. Velocities of atoms are scaled every 50 steps to keep the temperature constant.

The intensity of XANES can be approximated within the single-particle approximation as²¹

$$\mu \propto \sum_f \left| \left\langle \phi_f \left| \boldsymbol{\epsilon} \cdot \mathbf{r} + \frac{i}{2} (\boldsymbol{\epsilon} \cdot \mathbf{r})(\mathbf{k} \cdot \mathbf{r}) \right| \phi_c \right\rangle \right|^2 \delta(\hbar\omega - E_f + E_c), \quad (1)$$

where $\hbar\omega$, \mathbf{k} and $\boldsymbol{\epsilon}$ are the energy, the wave number vector and the polarization-direction vector of the incident X ray, and \mathbf{r} is the position operator. E_c is the total energy of the initial ground-state system, including core electrons, and E_f is the total energy of the final system excited by X-ray irradiation, containing an excited electron and a core hole. ϕ_c and ϕ_f are conceptually many-body wave functions of all the electrons in the initial and final systems, while practically we use one-particle wave functions of a core orbital and an excited state of the final system, respectively. Within the dipole approximation, the above equation can be rewritten as

$$\mu \propto \sum_f \left[\epsilon_x^2 |\langle \phi_f | x | \phi_c \rangle|^2 + \epsilon_y^2 |\langle \phi_f | y | \phi_c \rangle|^2 + \epsilon_z^2 |\langle \phi_f | z | \phi_c \rangle|^2 \right] \delta(\hbar\omega - E_f + E_c), \quad (2)$$

where $\epsilon_x^2 + \epsilon_y^2 + \epsilon_z^2 = 1$. For a polarized X-ray beam, the direction-dependent (x , y , and z) spectra can be theoretically simulated by calculating the corresponding polarization vector $\boldsymbol{\epsilon}$. Unless otherwise noted, theoretical spectra are averaged over all directions, *i.e.*, $\epsilon_x^2 = \epsilon_y^2 = \epsilon_z^2 = 1/3$. For E_f and ϕ_f in calculations of Co K -edge XANES spectra, the core-hole effects are incorporated via a large supercell containing a target Co atom with the PAW

pseudopotential constructed for an excited atom with a core hole in the $1s$ orbital.¹⁰ For the bulk LiCoO_2 system, we use a hexagonal supercell of $3 \times 3 \times 1$ unit cells containing 108 atoms so as to prevent unphysical strong interactions among the excited atoms with a core hole in repeated cells, as reported previously.¹¹ For the LiCoO_2 -electrolyte interface system, we use a supercell common with the FPMD simulations explained later. The absolute transition energy $E_f - E_c$ can be quantitatively obtained within the PAW-GGA framework via the total-energy difference between the excited and ground state of a large supercell including a core hole with supplement calculations of a free atom to deal with core electrons.¹⁰

III. RESULTS

A. Constructing an interface model

Optimized structural parameters of LiCoO_2 with layered rocksalt structure (space group $R\bar{3}m$ and No. 166) are $a = b = 2.840$ and $c = 14.190$ Å, which are in good agreement with experimental values $a = b = 2.816$ and $c = 14.054$ Å,²² and other theoretical ones¹² with a hybrid functional (HSE06)²³ for exchange-correlation. The LiCoO_2 $\{110\}$ surface has been reported as one of the lowest-energy nonpolar surfaces.^{24,25} SEM (scanning electron microscopy) observation showed that the $\{110\}$ surface is actually present as a significant proportion of LiCoO_2 crystal surfaces, and the surface reactivity with SO_2 and CO_2 was investigated theoretically.²⁶ Thus, we deal with a $\{110\}$ surface model. Since an orthorhombic supercell, in which one of lattice parameters is 14.190 Å, is substantially large for surface and interface models, we construct a smaller monoclinic supercell consisting of 8 layers as shown in Fig. 1. The x axis is perpendicular to the surface and the y and z axes are in plane with the surface. The thickness of a vacuum region is set to be 12 Å. In this model, Co layers are perpendicular to the surface plane. The \mathbf{k} point grid is set as $1 \times 2 \times 2$ in the full Brillouin zone for self-consistent calculations, and $2 \times 4 \times 4$ for density of states (DOS) and XANES calculations. After all atomic positions in the surface slab are optimized, the interlayer distance between layers 1 and 2 is 1.332 Å, which is shorter than that between layers 3 and 4 in the bulk-like region, 1.414 Å.

We analyze the orbital-decomposed partial density of states (PDOS) for Co d for each layer, as shown in Fig. 2. Only surface Co d PDOS is significantly different from those

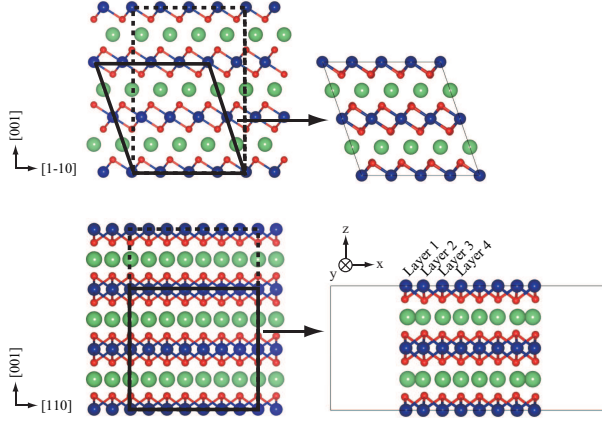


FIG. 1: Top (upper panel) and side (lower panel) views of a $\{110\}$ surface slab of LiCoO_2 . Solid lines indicate a monoclinic supercell, while dashed lines indicate an orthorhombic supercell. A dark blue ball denotes a Co atom, small red one an O atom, and green one a Li atom.

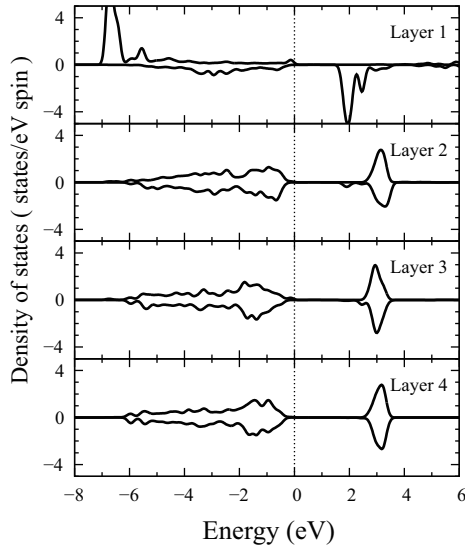


FIG. 2: Co d PDOS in each layer of the LiCoO_2 $\{110\}$ surface slab. The labels for layers are the same as in Fig. 1. The top of the valence band is chosen as zero energy.

for other layers. In bulk LiCoO_2 , each Co atom is coordinated with six equivalent oxygen atoms, and bond lengths of Co-O are 1.944 Å. In the PDOSs of layers 2, 3 and 4, six d electrons per Co^{3+} ion fully occupy t_{2g} states of up and down spin, resulting in $S = 0$. At the surface, the coordination of Co is reduced to four, two long in-plane bonds (1.993 Å)

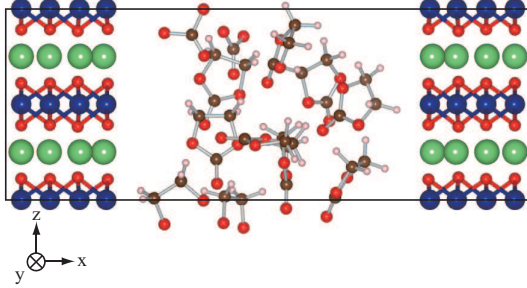


FIG. 3: Supercell for interfaces between LiCoO_2 and liquid EC. The definition of x , y , and z axes is the same as that in Fig. 1.

and two short back bonds (1.841 Å). These changes result in the resolve of degeneracies in t_{2g} and e_g states. In the PDOS of the surface Co^{3+} ion, five d electrons fully occupy the d states of up spin, and remaining one electron occupies the d state of down spin, resulting in $S = 2$ as discussed in ref 24.

To model a liquid EC ($\text{C}_3\text{H}_4\text{O}_3$) electrolyte, we prepare a monoclinic cell. The lengths of a and b axes are common with the LiCoO_2 surface supercell shown in Fig. 1, and the length of c axis is set to reproduce experimental density of 1.32 g/cm^{327} for ten EC molecules. We put EC molecules at equally spaced sites as an initial configuration, and optimized atomic positions by performing a FPMD simulation in 4000 steps at 500 K, and finally obtained the liquid EC model.

To construct a LiCoO_2 -EC interface model, we put the monoclinic box of the liquid EC at the position of 2 Å from the surface of the LiCoO_2 slab for both sides, resulting in two inequivalent interfaces in the supercell as shown in Fig. 3, where total 228 atoms are contained. To smooth these interfaces, we performed a full FPMD simulation of the supercell at 200 K. Chemical reactions were observed only at one-side interface, which will be analyzed in the next section.

B. FPMD simulation results

We performed a FPMD simulation of the interface model in 3000 steps at 600 K. We kept the temperature higher than that at which LIBs are usually operated to accelerate chemical reactions. We observed following behaviors as shown in Fig. 4. (i) An oxygen atom O_1 of

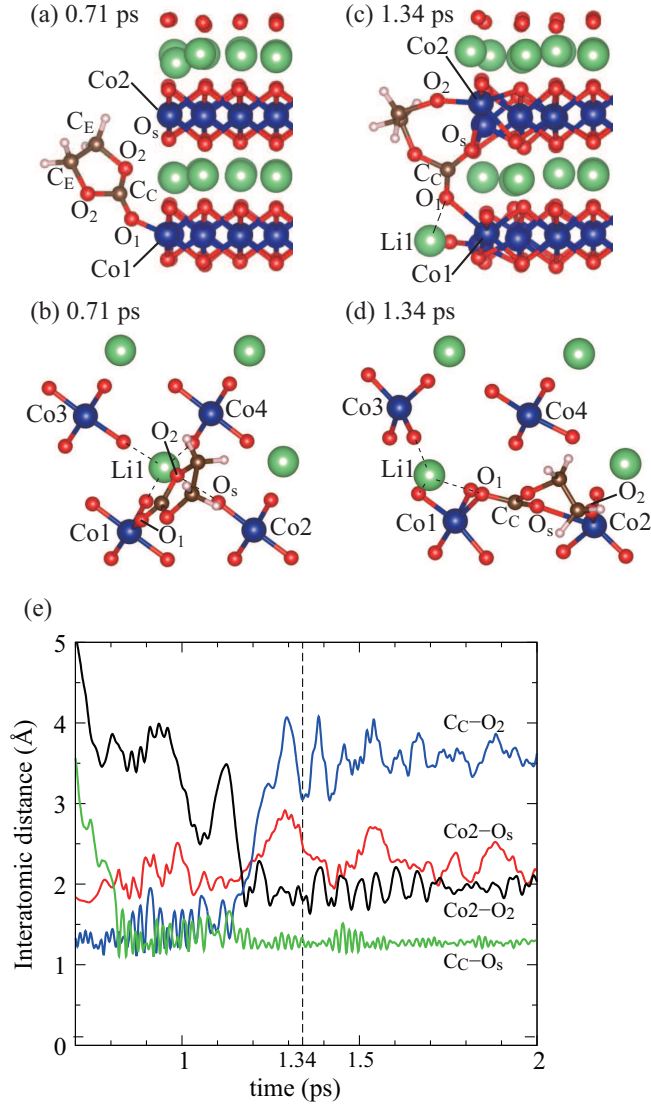


FIG. 4: Snapshots of the chemical reactions at a LiCoO₂-EC interface at (a)(b) 0.71 ps and (c)(d) 1.34 ps. O₁ atom was absorbed to Co1 atom. The bonds to Li1 are shown by dotted lines. (e) Time evolution of interatomic distances related to the ring-cleavage reaction of EC.

EC is absorbed to a surface Co1 atom. (ii) A carbonyl carbon atom C_C of EC is absorbed to a surface oxygen atom O_s. (iii) An oxygen atom O₂ of EC is absorbed to a surface Co2 atom. (iv) C_C-O₂ bond in EC is broken, *i.e.*, the ring structure of EC is cleaved. (v) A surface Li ion is released. To understand details of the ring-cleavage reaction of EC, we analyzed the interatomic distances from 0.7 ps to 2.0 ps as shown in Fig. 4(e). Around 0.8 ps, the distance between C_C of EC and the surface oxygen atom O_s bonded to the surface Co2 atom

decreases (the reaction (ii)). Around 1.15 ps, drastic changes of interatomic distances can be seen. The distance between the surface Co2 atom and the O₂ atom of EC decreases, and the distances between the C_C and O₂ atoms and between the Co2 and O_s atoms increase. In addition, the width of the oscillation of C_C-O_s bond decreases. These results indicate that the reactions (iii) and (iv) occur simultaneously. At 1.34 ps, the distance between the Co2 and O_s atoms is 2.425 Å, which is much longer than that in the bulk LiCoO₂, 1.944 Å, indicating that the coordination of Co2 remains to be four by removal of O_s and addition of O₂. Note that the coordination of Co1 kept five by the bond with O₁. After 2.0 ps, no drastic changes were seen. In Figs. 4(c) and (d) at 1.34 ps, the released Li ion (Li1) is bonded to three oxygen atoms, O bonded to Co3, O bonded to Co1, and O₁ of EC, and the interatomic distances to these oxygen atoms are 1.795, 2.063, and 2.307 Å, respectively. The valence state of this Li ion was unchanged from +1. Other three surface Li ions kept their initial positions with oscillations. Thus, it can be thought that the the release of Li was caused by the attractive interaction between the Li1 atom and the O₁ atom absorbed to the surface Co1. Along with this release, the oxygen atom bonded to Co3 largely moved from its initial position. The averaged interlayer distance between layers 1 and 2 at 0.71 ps is 1.333 Å, similar to that for the clean surface model, and that at 1.34 ps is 1.417 Å. This indicates that surface Co ions moved toward the liquid region by the absorption of EC. These reactions are observed at only one-side interface in the interface supercell, and we did not observe a resolution of EC to CO₂.

The solid-electrolyte interphase (SEI) formed near anode surfaces through the reductive decomposition of the electrolyte plays a crucial role in the stability and durability of LIBs. Thus, first-principles calculations of electrolyte decompositions have been extensively performed, and two decomposition reactions for the bond cleavage of an EC molecule have been proposed:^{5,28,29} one is the cleavage at the ethylene carbon C_E-O₂ bond, and the other is the cleavage at the carbonyl carbon C_C-O₂ bond. Ushirogata *et al.* carried out constrained FPMD in the framework of Blue-moon ensemble for the decomposition barriers, and concluded that the bond cleavage of C_E-O₂ occurs under one-electron reduction condition of EC and the bond cleavage of C_C-O₂ is unfavorable.⁵ However, these reduction reactions donating an electron to a molecule should not occur near cathode. The O₁ atom can be absorbed to a surface Co atom which is positively charged since O₁ of EC is more negatively charged than O₂. We analyzed the charge-density difference by absorption of the O₁ atom

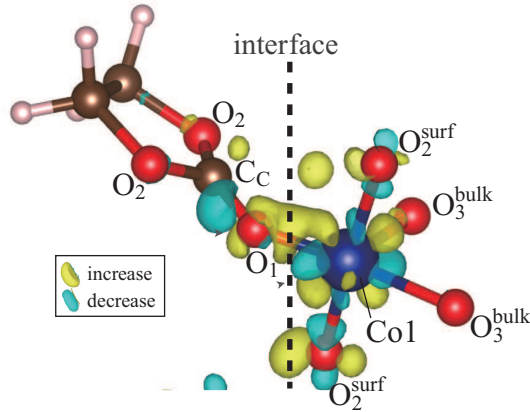


FIG. 5: Charge transfer at the LiCoO₂-EC interface at 0.71 ps. The charge transfer was obtained as the difference between the final charge-density distribution of the interface configuration and the superposition of the two charge distributions obtained for each molecular and surface systems by removing each half of the interface configuration. Yellow and blue mean charge accumulation and charge depletion, respectively. O₂^{surf} and O₃^{bulk} denote surface twofold and bulk threefold oxygen atoms, respectively.

in EC to the LiCoO₂ surface as shown in Fig. 5. By forming a bond between O₁ and Co1, the charge density is largely redistributed at the interface. We can see the charge-density reduction on C_C-O₁ bond. Thus C_C can be easily absorbed to a surface O atom, leading to the C_C-O₂ bond cleavage, associated with simultaneous absorption of O₂ onto Co2. The coordination of the surface Co1 atom is changed from four to five, and the symmetry of *d* orbitals is changed. One electron of *e_g* state of up spin for the surface fourfold Co³⁺ ion moves to *t_{2g}* state of down spin, resulting in *S* = 1. These changes affect the charge density of neighboring O atoms. Bonding 2*p* electrons on surrounding Co1-O₂^{surf} bonds are reduced and non-bonding electrons are increased. The increase of non-bonding O₂^{surf} 2*p* electrons implies the increase of chemical reactivity of these atoms in the direction normal to the surface. Thus the released Li1 ion is bonded to one of O₂^{surf} at 1.34 ps. From the analysis of Co *d* PDOS, we confirmed that the valence state 3+ of surface Co atoms did not change during the MD simulation of the interfacial reactions.

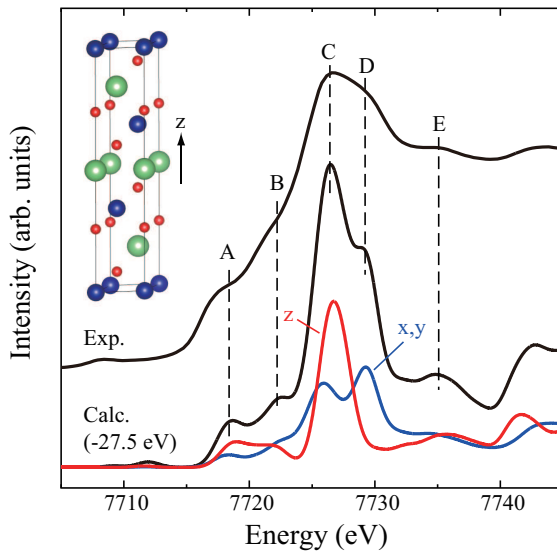


FIG. 6: Calculated Co K -edge spectrum for bulk LiCoO_2 in comparison with an experimental one.² The calculated absolute transition energy was adjusted to the experimental one by the shift of -27.5 eV. Polarized spectra are also plotted by blue and red lines.

C. XANES simulation results

Figure 6 shows the calculated Co K -edge spectrum for bulk LiCoO_2 in comparison with an experimental one.² The calculated spectrum is shifted to lower energy by 27.5 eV to match the highest peak of the experimental one. We introduced one core hole as two halves of both spins in calculating the absolute transition energy in our code,¹⁰ while this treatment leads to overestimation of the transition energy by about 30 eV for LiCoO_2 than the introduction of one core hole to a specific spin state as pointed out in ref 12. The calculation sufficiently reproduced spectral features (labeled as A-E in the figure) of experimental results. The layered rocksalt structure of LiCoO_2 induces orientation-dependent Co K -edge spectra, as observed by polarized X-rays with the electric field parallel to x , y or z axis. This can be obtained by Eq. (2) with each polarized-direction vector ϵ . The $(\epsilon \parallel x)$ and $(\epsilon \parallel y)$ spectra match perfectly, resulting in the two components as $(\epsilon \parallel x, y)$ and $(\epsilon \parallel z)$. A clear difference can be seen for the major peaks C and D. The $(\epsilon \parallel z)$ spectrum consists of a single peak,

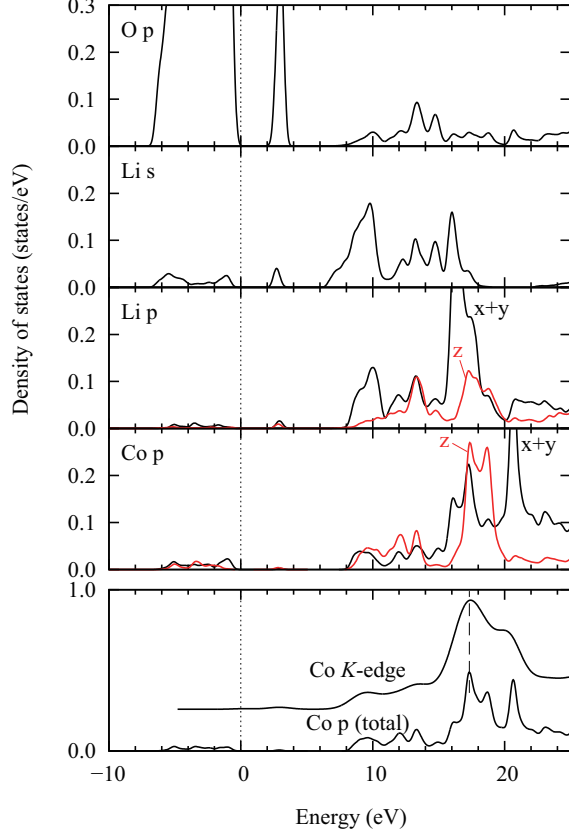


FIG. 7: Unoccupied PDOSs for bulk LiCoO_2 in comparison with the calculated Co K -edge spectrum. O p , Li s , Li p_{x+y} , Li p_z , Co p_{x+y} , and Co p_z components are plotted.

while the ($\epsilon \parallel x, y$) spectra consist of double peaks. Thus, the highest peak C is composed of ($\epsilon \parallel x, y$) and ($\epsilon \parallel z$), and the second highest peak D is composed of only ($\epsilon \parallel x, y$). In order to interpret the XANES spectra compared to the electronic structure, unoccupied PDOSs of Co, Li, and O in the bulk are shown in Fig. 7. Spectral features of xy -component of the Co K -edge spectrum match the Co p_x and p_y PDOSs, and those of z -component match the Co p_z PDOS, since the Co K -edge spectrum should mainly come from Co $1s \rightarrow 4p$ transition. Co p_z hybridizes strongly with Li p_z at 17-19 eV. Co p_{xy} strongly hybridize with Li p_{xy} at 16-17 eV, while slightly hybridize at 21 eV. These results indicate that the highest peak C of the Co K -edge spectrum mainly originates from Co p_z -Li p_z hybridization, while the shoulder of this peak is caused by Co p_{xy} -Li p_{xy} hybridization, and that the second highest peak D mainly originates from only Co p_{xy} . The present orientation dependence of the XANES spectra and the comparison with the PDOSs are consistent with the previous

theoretical^{11,12,14} and experimental¹⁴ results.

Since CoO is widely used as a reference material with valence state 2+ for Co, the Co d and p PDOSs and the Co K -edge spectrum for LiCoO₂ are compared with those for CoO in Fig. 8. As for the d PDOS, LiCoO₂ and CoO show quite different features. For Co²⁺ ion of CoO, five of seven d electrons fully occupy the d states of up spin, and remaining two d electrons occupy the d states of down spin, resulting in $S = 3/2$.³⁰ On the other hand, the PDOSs of Co p_{xy} in LiCoO₂ and Co p in CoO are similar to each other in Fig. 8(b). It can be clearly seen that the calculated Co K -edge spectrum of CoO has the two high peaks similarly to the Co p PDOS. In LiCoO₂, the Co p_z PDOS has peaks in the valley between the two high peaks of the Co p_{xy} PDOS as also shown in Fig. 7. These results lead to an important point that the origins of the highest peaks in the Co K -edge spectra of LiCoO₂ and CoO are different. For LiCoO₂, the highest peak comes from Co p -Li p hybridization as analyzed in Fig. 7, while that for CoO comes from Co p -Co p hybridization.

Figure 9 shows calculated Co K -edge spectra from each layer of the LiCoO₂ {110} surface, while only the averaged spectra within a depth of a few nanometers can be obtained experimentally. Only the surface-layer Co shows a quite different spectrum, compared to the inner or bulk layers, which is consistent with the Co d PDOSs in Fig. 2. The spectral features of layer 1 are broadened, which is consistent with the experimental results.³ The number of neighboring Li ions for Co ions decreases at the surface, which should induce a remarkable decrease of the z component of the peak C. Interestingly, the energy position of the peak C is common among all the layers, while the peak D of layer 1 is located at a slightly higher energy level. As discussed above, the peak D originates from Co p_{xy} hybridization in Co layers. The number of neighboring Co ions for surface Co ions decreases in the x direction, while not in the y direction. This causes the decrease of Co p_x hybridization and the increase of Co p_y hybridization, resulting in the shift to lower energy of the x component and to higher energy of the y component of the peak D. The previous theoretical simulations of the Co K -edge spectra for bulk Li_{1-x}CoO₂ during the Li deintercalation process showed that the peak D was unchanged because of no significant local environment changes in Co layers by the Li removal.¹⁴

Figure 10 shows averaged Co K -edge spectra of surface Co atoms in the configurations during the FPMD of the LiCoO₂-EC interface. Spectral differences from the clean surface are rather small at 0.71 ps, while at 1.34 ps there occur remarkable changes in the main

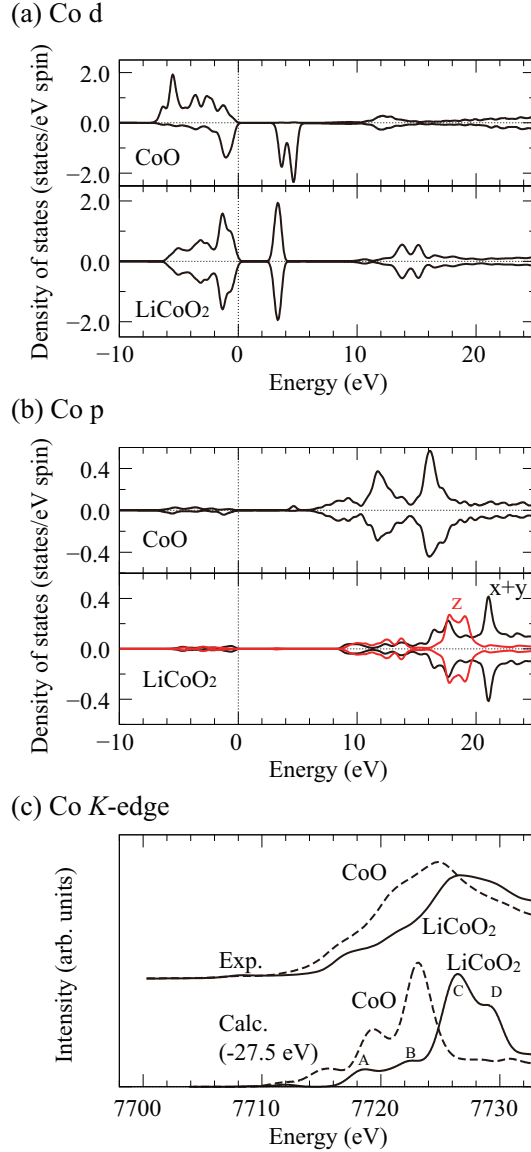


FIG. 8: Comparison of Co (a) *d* and (b) *p* PDOSs, and (c) *K*-edge XANES spectrum, for bulk LiCoO₂ with those for bulk CoO. Calculated *K*-edge spectra are shifted to lower energy by 27.5 eV as in Fig. 6, and compared with experimental spectra.²

region, namely around the peaks B, C and D. In Fig. 10 (b), we can see a remarkable decrease at the highest peak C and a remarkable increase around the peak B as a shoulder. These changes are quite similar to those observed in the *in-situ* XANES observation of LiCoO₂ under electrolyte soaking.³ In Fig. 10 (c), we show the Co *K*-edge spectrum from each surface Co atom at 1.34 ps. As discussed above, Co1 is in $S = 1$ spin state with five

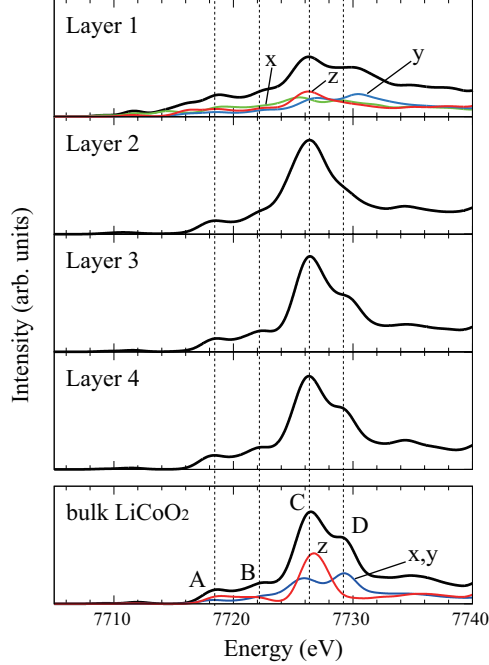


FIG. 9: Calculated Co K -edge spectra from each layer of the LiCoO_2 $\{110\}$ surface in comparison with that for bulk. All spectra are shifted to lower energy by 27.5 eV as in Fig. 6, and the definition of the x , y , and z axes and the labels for layers are the same as in Fig. 1

coordination, and Co_2 , Co_3 and Co_4 are in $S = 2$ spin state with four coordination. This indicates that the valence state of all the surface Co ions is $3+$. However, the spectrum of each Co atom shows substantial differences from that in the clean surface, depending on the local environment. The changes in the spectra for Co_1 and Co_2 newly bonded to oxygen atoms in the broken EC molecule are remarkable. Co_3 is not directly involved in the bond formation with the EC molecule, while the spectrum changes are also remarkable. The decrease and the shift to the lower energy can be seen for the z component of the peak C in these Co atoms. Especially the changes for Co_1 are remarkable, resulting in the increase in the peak B. For Co_4 , the change in the local environment is small except for the increase of the Li_1 - Co_4 distance from 2.854 to 5.063 Å, which seems to induce slight changes in the z component of the peak C similar to the other Co atoms. Interestingly, this shift is opposite to that for Li de-intercalation from the bulk LiCoO_2 .¹⁴ Along with the observed chemical reactions, O and Li atoms around Co_1 , Co_2 , and Co_3 are largely moved, resulting in large changes in the z component around the peak A. In the present supercell, the x axis

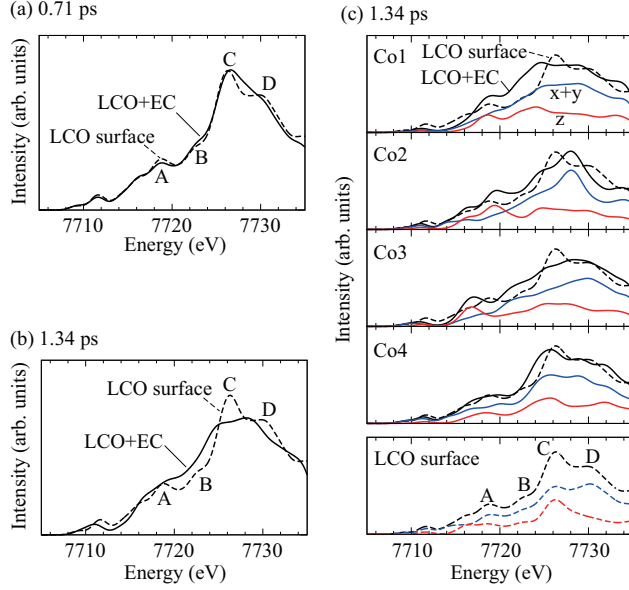


FIG. 10: Calculated averaged K -edge spectra for surface Co atoms of the LiCoO_2 -EC interface at (a) 0.71 ps and (b) 1.34 ps, and (c) individual K -edge spectra from each surface Co atom at 1.34 ps in comparison with those of the clean surface. All spectra are shifted to lower energy by 27.5 eV as in Fig. 6, and the labels for atoms are the same as in Fig. 4.

is perpendicular to the surface and the y axis is in plane with the surface. Thus, the local environment is greatly changed in the x direction for each surface atom. The Co2 ion moved away from the Co layer, which greatly reduces the Co p -Co p hybridization, inducing the narrowing Co- p PDOSs in Fig. 8. This should be the origin of the sharp peak in the $x + y$ curve of Co2 at the energy level between the peaks C and D of the clean-surface spectrum in Fig. 10 (c). It is apparent that the local structural changes around surface Co ions induced by the interfacial reactions with the EC electrolyte, such as bond formation with oxygen atoms in the molecule, displacements of surface Co and surrounding oxygen atoms, and surface Li release, should induce remarkable changes in the surface-Co K -edge spectra.

IV. DISCUSSION

In the present study, we investigated interfacial reactions between a LiCoO_2 electrode and a liquid EC electrolyte by FPMD for the first time. For the LiCoO_2 $\{110\}$ surface with a liquid EC, we observed a strong chemical reaction as the absorption of oxygen atoms of

EC to surface Co ions, involving ring opening of EC, followed by coordination changes of Co and surface-Li release, while we did not observe the reduction of Co^{3+} to Co^{2+} or the formation of local CoO-like configurations. In the calculated Co K -edge XANES spectra during the FPMD, remarkable changes for surface Co ions bonded with oxygen atoms of EC are consistent with those in experimental spectra under electrolyte soaking. From these results, the local environmental changes of surface Co^{3+} ions without the reduction to Co^{2+} can possibly lead to the experimental spectrum changes. We performed only one FPMD simulation, but at least, our results are of fundamental significance as an evidence of the alternative interpretation for the experimental spectrum changes.

The present study does not necessarily deny possibilities of other chemical reactions or other origins of XANES spectra changes. The presence of other components in an electrolyte such as DEC and Li salts, and the presence of defects or steps on the LiCoO_2 surface may induce other features of chemical reactions. About the surface orientation, typical nanosized LiCoO_2 particles are dominated by the $\{100\}$ surface, which is not active for Li (de)intercalation, and the $\{104\}$ -surface energy is theoretically lower than that of $\{110\}$,^{24,25} because of five coordination for Co^{3+} ions on the $\{104\}$ surface, compared to the four coordination on the $\{110\}$ surface. In the sample used for TRF-XAS observation in ref. 3, the c -axis of LiCoO_2 was tilted from the normal of the substrate and the in-plane orientation was random, but the coordination of surface Co ions was not clear. It can be thought that the reactivity of the $\{110\}$ surface is higher than that of the $\{104\}$ surface, which may lead to the present spontaneous reactions during a rather short period of the FPMD simulation in addition to the effect of slightly high temperature. Of course, it is desirable to perform further FPMD simulations dealing with various kinds of LiCoO_2 surfaces and electrolytes with multiple components in the future. However, note that the present phenomenon observed in the FPMD and XANES simulations has some generality as follows; one oxygen atom is negatively charged in EC, leading to the adsorption onto a positively-charged surface Co atom, and the local environment change of the surface Co atom induces remarkable electronic-structure change, due to the sensitivity of $3d$ states. This may possibly occur as initial reactions in any systems of LiCoO_2 surfaces in contact with EC in a liquid state.

As mentioned in Introduction, the origin of experimental spectrum changes by electrolyte soaking was attributed to the reduction of Co^{3+} to Co^{2+} in ref. 3. This is because DFT calculations suggested the stability of antisite Co ions at Li sites in bulk LiCoO_2 for a low

oxygen chemical potential by the contact with the electrolyte. The local structure of an antisite Co ion should be similar to CoO with Co^{2+} , and if the $\text{Co}^{2+}/\text{Co}^{3+}$ ratio at/near the surface increases, the heights of the peaks B and C in the K -edge spectrum should increase and decrease, respectively, as expected from Fig. 8(c). However, there remain several ambiguities in this argument of ref. 3. The formation of local CoO-like configurations via antisite Co ions should involve alternative Li_2O -like configurations and/or the removal of oxygen or Li ions. There are no clear pictures on the procedure of such structural evolution at LiCoO_2 -electrolyte interfaces. Furthermore, there have been no theoretical simulations of XANES from such local structural changes.

V. CONCLUSION

We performed a FPMD simulation of the interface between a LiCoO_2 cathode and a liquid EC electrolyte in order to clarify the chemical reactions at this interface. We observed following behaviors: (i) an oxygen atom O_1 of EC is absorbed to a surface Co atom, (ii) a carbonyl carbon atom C_C of EC is absorbed to a surface oxygen atom, (iii) an oxygen atom O_2 of EC is absorbed to a nearby surface Co atom, (iv) C_C - O_2 bond in EC is broken, i.e. the ring structure of EC is cleaved, and (v) a surface Li ion is released. The reactions (iii) and (iv) occur simultaneously. Surface Co ions moved toward the liquid side by the absorption of EC, and the numbers and directions of coordinated oxygen ions around the surface Co ions were substantially changed. We also performed theoretical XANES simulations of Co K -edge for the configurations during the FPMD. The surface Co ions having the bond with an oxygen atom in the EC molecule showed remarkable changes in the Co K -edge spectra, similar to the experimental changes. Our results indicate that local environmental changes of surface Co ions via reactions with a liquid EC can possibly lead to the experimental spectrum changes, without the reduction of Co^{3+} to Co^{2+} . We can conclude that *in-situ* theoretical XAS simulations, namely effective combinations between XANES and FPMD simulations, are effective to understand *in-situ* experimental XAS results of chemical reactions or dynamical systems.

Acknowledgements

We would like to thank S. Tanaka and T. Ohwaki for helpful discussions. This work was supported by MEXT Kakenhi 25820355 and 26249092. All of the crystal structures were drawn using the VESTA software.³¹

References

- * Electronic address: tamura.tomoyuki@nitech.ac.jp
- ¹ B. Y. Liaw and R. Kosteci, *Electrochem. Soc. Interface* **3**, 41 (2011).
 - ² A. Ito, Y. Sato, T. Sanada, M. Hatano, H. Horie, and Y. Ohsawa, *J. Power Sources* **196**, 6828 (2011).
 - ³ D. Takamatsu, Y. Koyama, Y. Orikasa, S. Mori, T. Nakatsutsumi, T. Hirano, H. Tanida, H. Arai, Y. Uchimoto, and Z. Ogumi, *Angew. Chem. Int. Ed.* **51**, 11597 (2012).
 - ⁴ T. Ohwaki, M. Otani, T. Ikeshoji, and T. Ozaki, *J. Chem. Phys.* **136**, 134101 (2012).
 - ⁵ K. Ushirogata, K. Sodeyama, Y. Okuno, and Y. Tateyama, *J. Am. Chem. Soc.* **135**, 11967 (2013).
 - ⁶ S. Ogata, N. Ohba, and T. Kouno, *J. Phys. Chem. C* **117**, 17960 (2013).
 - ⁷ T. Mizoguchi, M. Sakurai, A. Nakamura, K. Matsunaga, I. Tanaka, T. Yamamoto, and Y. Ikuhara, *Phys. Rev. B* **70**, 153101 (2004).
 - ⁸ T. Yamamoto, T. Mizoguchi, and I. Tanaka, *Phys. Rev. B* **71**, 245113 (2005).
 - ⁹ C. Gougoussis, M. Calandra, A. Seitsonen, C. Brouder, A. Shukla, and F. Mauri, *Phys. Rev. B* **79**, 045118 (2009).
 - ¹⁰ T. Tamura, S. Tanaka, and M. Kohyama, *Phys. Rev. B* **85**, 205210 (2012).
 - ¹¹ A. Juhin, F. de Groot, G. Vankó, M. Calandra, and C. Brouder, *Phys. Rev. B* **81**, 115115 (2010).
 - ¹² Y. Koyama, H. Arai, , Z. Ogumi, I. Tanaka, and Y. Uchimoto, *Phys. Rev. B* **85**, 075129 (2012).
 - ¹³ T. Tamura, T. Ohwaki, A. Ito, Y. Ohsawa, R. Kobayashi, and S. Ogata, *Modelling Simul. Mater. Sci. Eng.* **20**, 045006 (2012).

- ¹⁴ T. Okumura, Y. Yamaguchi, M. Shikano, and H. Kobayashi, *J. Mater. Chem.* **22**, 17340 (2012).
- ¹⁵ <http://www.qmas.jp>.
- ¹⁶ P. E. Blöchl, *Phys. Rev. B* **50**, 17953 (1994).
- ¹⁷ N. A. W. Holzwarth, G. E. Matthews, R. B. Dunning, A. R. Tackett, and Y. Zeng, *Phys. Rev. B* **55**, 2005 (1997).
- ¹⁸ G. Kresse and D. Joubert, *Phys. Rev. B* **59**, 1758 (1999).
- ¹⁹ J. P. Perdew, K. Burke, and M. Ernzerhof, *Phys. Rev. Lett.* **77**, 3865 (1996).
- ²⁰ V. I. Anisimov, J. Zaanen, and O. K. Andersen, *Phys. Rev. B* **44**, 943 (1991).
- ²¹ C. Brouder, *J. Phys.: Condens. Matter* **2**, 701 (1990).
- ²² J. Akimoto, Y. Gotoh, and Y. Oosawa, *J. Solid State Chem.* **141**, 298 (1998).
- ²³ J. Heyd, G. Scuseria, and M. Ernzerhof, *J. Chem. Phys.* **124**, 219906 (2006).
- ²⁴ D. Qian, Y. Hinuma, H. Chen, L.-S. Du, K. Carroll, G. Ceder, C. Grey, and Y. Meng, *J. Am. Chem. Soc.* **134**, 6096 (2012).
- ²⁵ D. Kramer and G. Ceder, *Chem. Mater.* **21**, 3799 (2009).
- ²⁶ N. Andreu, I. Baraille, H. Martinez, R. Dedryvère, M. Loudet, and D. Gonbeau, *J. Phys. Chem. C* **116**, 20332 (2012).
- ²⁷ A. Marquez, *Mater. Chem. Phys.* **104**, 199 (2007).
- ²⁸ Y. Wang, S. Nakamura, M. Ue, and P. B. Balbuena, *J. Am. Chem. Soc.* **123**, 11708 (2001).
- ²⁹ K. Leung and J. L. Budzien, *Phys. Chem. Chem. Phys.* **12**, 6583 (2010).
- ³⁰ M. J. Han, T. Ozaki, and J. Yu, *Phys. Rev. B* **73**, 045110 (2006).
- ³¹ K. Momma and F. Izumi, *J. Appl. Crystallogr.* **44**, 1272 (2011).